Hindawi
Advances in Civil Engineering
Volume 2019, Article ID 9537153, 11 pages
https://doi.org/10.1155/2019/9537153

Research Article

Experimental and Analytical Study on Mechanical Properties of High Rock Temperature Diversion Tunnel

Xianchun Yao,[1,2] Ning Li,[1,2] Kecheng Wan,[3] Gao Lv,[1,2] and Mingming He[1,2]

[1] *Institute of Geotechnical Engineering, Xi'an University of Technology, Xi'an, Shaanxi 710048, China*
[2] *State Key Laboratory Base of Eco-Hydraulic Engineering in Arid Area, Xi'an, Shaanxi 710048, China*
[3] *Power China Northwest Engineering Corporation Limited, Xi'an, Shaanxi 710065, China*

Correspondence should be addressed to Xianchun Yao; yxc@xaut.edu.cn

Received 16 January 2019; Revised 12 March 2019; Accepted 21 March 2019; Published 4 April 2019

Academic Editor: Flavio Stochino

The high temperature of rock used in different working conditions has a significant effect on the deformation characteristics and the mechanics of tunnel lining support structure. A test using a laboratory model is designed to study the quantitative relationship between the temperature difference and the support force. Through the laboratory model test, the strain and stress variation characteristics of the supporting structure of a water diversion tunnel under different surrounding rock temperatures and different water temperatures were simulated. The variation characteristics of the supporting structure under various working conditions, such as a different initial temperature field, different crossing water temperature of the diversion tunnel during runtime, and repairing period after the water is emptied, were analyzed. The relationship between the high-temperature difference between the inner and outer walls of the tunnel lining support structure and the internal temperature stress of the supporting structure was obtained and compared with the results from numerical experiments. The test results showed that a high circumferential tensile stress is created in the support structure of the high-temperature diversion tunnel due to the temperature difference between the inner and outer walls of the support structure caused by water going through the high-temperature diversion tunnel. The radial compressive stress increases by 45–50%, and the circumferential tensile stress increases by 40–60%. The results provide references for the design of the support structure in a high-temperature tunnel.

1. Introduction

The internal temperature of surrounding rock was found to reach 105°C when the high-temperature diversion tunnel located at Xinjiang, Uygur Autonomous Region, was constructed. However, the temperature of water that runs through the tunnel ranges from 5°C to 10°C. The inner and outer walls of the support structure will have a high temperature difference when the water runs. The study of the influence of high temperature differences on the stress state of the support structure is a new problem and challenge faced in the analysis and design of tunnel support structures.

In underground engineering problems that are affected by high temperatures, existing achievements and studies focus on the supporting structure and laws of high-temperature stress of surrounding rock caused by fire and radioactive substances [1–5]. Studies on stress problems caused by high temperature differences are few, especially in hydraulic tunnels [6–9]. In studying the temperature field distribution of the surrounding rock in a tunnel and its impact on the surrounding rock in the supporting structure, a relatively large amount of research work has focused on the cold region of the tunnel [10–13]. Studies of the influence of high geothermal temperature on the stability of surrounding rock in underground caves and the safety of supporting structures had not begun until two decades ago. The most typical study is the DECOVALEX project, which comprises of authoritative experts whose purpose was to evaluate the safety of caves under the high-radiant heat of nuclear waste at ultrahigh temperatures (600°C–800°C) [14–17]. However, laboratory model test research on the stress state of the supporting structure is rare when the tunnel is at a high temperature. A model test is an effective method to study the force characteristics and deformation regularity of a tunnel support structure. The current model test for the stress characteristics of a support structure focuses on structural stress and deformation. To determine the effect of the long-term heat load on the lining stability of nuclear spent fuel, Pacovsky et al. [18] conducted two tunnel liner model tests and found that a long-term thermal effect can lead to a serious reduction of lining stability. This is due to the deterioration of the strength of lining materials or the breakdown of the lining because of deformation. By testing an asymmetrical load model tunnel excavation, Lei et al. [19] systematically studied the destruction mechanism of the tunnel lining and surrounding rock, the structural stress and the variation rule, and the distribution of surrounding rock pressure under the effect of asymmetric load. To study the mechanical characteristics of the segmented lining structure of the TBM tunnel, Molins et al. [20] conducted an experiment on the Barcelona metro line 9 (L9) where they considered the real ground-structure interaction, developed a new tunnel testing method, and determined the related measurement values of the lining. These results provide strong evidence for the behavior of a reinforced concrete tunnel lining structure under a hard foundation.

The above research results do not involve water temperature and do not consider the change of tunnel lining stress caused by changes in water temperature. Research has rarely examined the internal force change characteristics and temperature and stress coupling of a tunnel support structure due to the temperature difference in the surrounding rock of the tunnel. With the development of water and electric lines in recent years, the problem of high ground temperature in western China has become increasingly prominent. It is necessary to carry out systematic research on the stability problems and structural characteristics of the surrounding rock in the cave. Based on this, the model test is adopted to simulate the relationship between the temperature difference between the inner and outer walls of the lining support structure. The relationship between the high temperature difference between the inner and outer walls of the tunnel lining support structure and the internal temperature stress of the supporting structure is obtained.

In this paper, a mortar annular prefabricated body is used to simulate the tunnel support structure, and an indoor heating model is used to simulate the different temperatures of the surrounding rock mass of the tunnel. By changing the temperature of the electric heating coil outside the mortar annular preform, the different surrounding rock temperatures of the diversion tunnel are simulated. The different water temperatures of the tunnel during the operation period are simulated by changing the temperature of the water in the prefabricated body. Based on the characteristics of temperature and strain and stress changes of the tunnel lining structure under different working conditions and different temperature schemes, the variation characteristics of the supporting structure under different working conditions are analyzed and compared with numerical experiments. The quantitative relationship between the high temperature difference between the inner and outer walls of the tunnel lining support structure and the internal temperature stress of the supporting structure is obtained.

Based on the high geothermal temperature diversion tunnel of the hydropower station in Xinjiang, China, the maximum temperature of the local surrounding rock detected in the borehole reaches 105°C, while the water temperature during operation is only 0–10°C. This high temperature difference between the surrounding rock and water will have a negative impact on the supporting structure's force state. To select a reasonable design method, construction protocol, and operation of the program, it is necessary to fully grasp the relationship between the high temperature difference between the inner and outer walls of the tunnel lining support structure and the internal temperature stress of the supporting structure. The field conditions are extremely poor, and the existing test instruments are not capable of withstanding a long-term high-temperature environment. Therefore, in order to obtain the relationship between the temperature difference and the stress of the lining structure, a laboratory test model method is reasonable and effective.

2. Design of Indoor Model Test Program

2.1. The Size and Production of the Model. According to existing literature [21, 22], the laboratory test is geometrically similar to the support structure of the #2 high-temperature rock test tunnel in the Xinjiang Hydropower Station by a ratio of 1 : 10. The size of the model is shown in Figure 1.

Considering the strength level of concrete in the test tunnel and the requirements of surface roughness and smoothness for the lining model, M25 mortar was used to make a model of the support structure. M25 is mixed at a proportion of mass : cement : river sand = 1 : 3 : 0.52. The test cement is ordinary silicate cement (PO32.5) from Qin ling, Shaanxi, and all the indices conform to the specification for "GB 175-2007 Common silicate cement." The sand is medium sand obtained from the Ba River in Xi'an with a fineness modulus of $\mu_f = 2.9$ and good gradation. A small mortar block with the same mixing proportion as the lining model is made as a carrier for the strain gauge to be affixed, and a small mortar block is buried in the support model later. To increase the bond between the small mortar block and the support model mortar and to ensure that the deformation of the small mortar block and the lining model is consistent, grooves are made on the side and bottom of the small mortar block. The size of the small mortar block is $70 \times 30 \times 20$ mm, and the form is shown in Figure 2. The paste of the strain gauge and packaging of insulation glue are shown in Figure 3. A BA120-6BA150 (11) biaxial foil strain gauge is selected for this test, where there are two mutually perpendicular sensitive gates on the substrate of the same piece in the strain gauge. It is used to measure the strain in two mutually perpendicular directions at the same observed point of the object. The strain gauge style and the main technical parameters are shown in Figure 4 and Table 1. The strain gauge is a three-tier uniform layout and set along the axis of the lining model; the layout is shown in Figure 5.

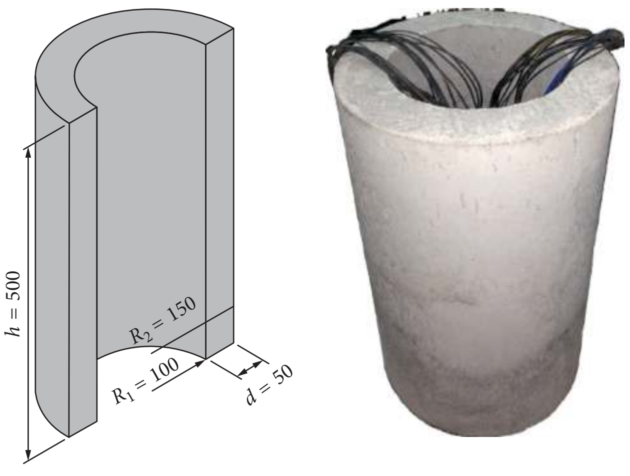

(a) (b)

Figure 1: Size of the lining structure model (unit: mm).

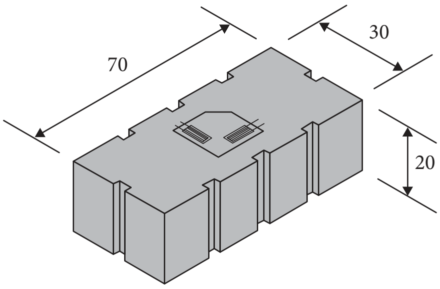

Figure 2: Size of the mortar brick (unit: mm).

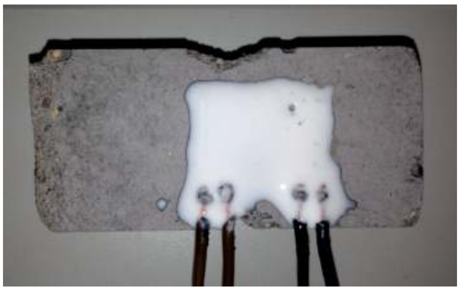

Figure 3: Adhesion and capsulation of the strain gauge.

2.2. Temperature Loading Method and Scheme.

In the test, the temperature of the lining rock was simulated by heating a customized stainless-steel mica using an electrothermal cycle. Mica is used for insulation, and a Ni–Cr alloy heating wire is used for heating the element; the outer layer is made of stainless steel for conducting the heat; and the diameter is 32 cm, and the height is 50 cm. There are four fixing screws on the side of the electrothermal cycle to adjust the diameter of the electrothermal cycle as needed to adapt to the model size. The overall power of the electrothermal cycle is 7.6 kW, as shown in Figure 6.

According to the field test data, it can be seen that the water temperature of the hydropower tunnel during the year is approximately 0°C–10°C. Therefore, it was determined that the control temperature of cold water under low temperature would be 0°C and 10°C. Water at 0°C is a mixture of ice and water and is used to simulate the winter water temperature and inlet water temperature of the tunnel; the outlet water temperature of the tap is controlled at 10°C, and it is used to simulate the summer water temperature. A complete test process is as follows: the electrothermal cycle is heated, and the support structure model is warmed; the electrothermal cycle is maintained at the set temperature, the model is maintained at a stable temperature; the electrothermal cycle is maintained at the set temperature, and the model is injected into the cold water; the electrothermal cycle is maintained at the set temperature, and the cold water is discharged. This process is shown in Figure 7.

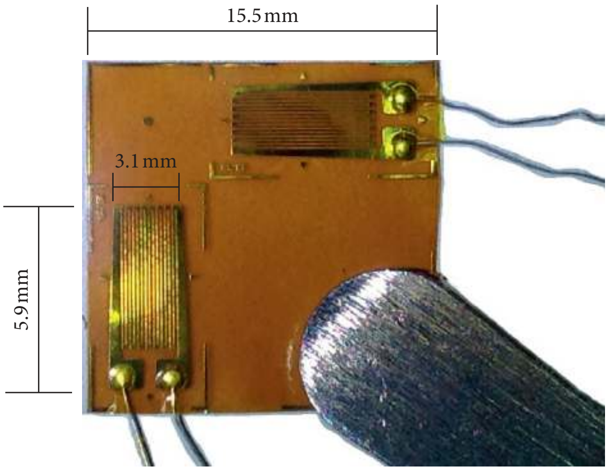

Figure 4: Strain gauge and sensitivity gate.

2.3. Data Measurement and Recording.

The DH3816 static strain test system from Dong hua, Jiangsu, is used to collect strain data. The system has the advantages of high sensitivity, low drift, and multipoint sampling. It can be used for the multipoint strain test and multipoint static stress and strain caused by factors such as compressive stress, force, and temperature. The test process is shown in Figure 8.

Table 1: Technical parameter of the strain gauge.

Resistance (Ω)	Sensitivity coefficient	Sensitive grid size (mm)	Base size (mm)	Strain limit
120.2 ± 0.3	2.13 ± 1%	5.9 × 3.1	15.5 × 15.5	2%

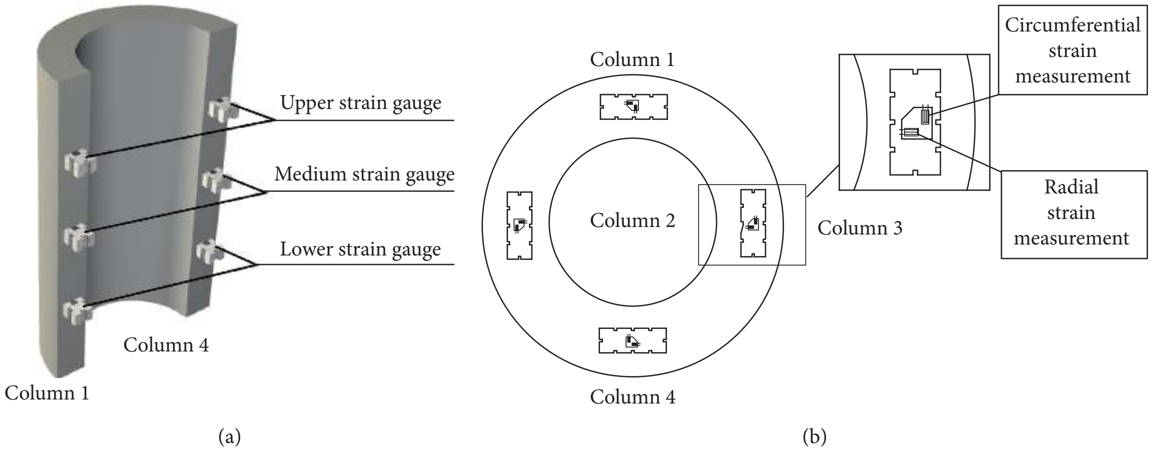

Figure 5: Arrangement of the strain gauge.

Figure 6: Electric heating equipment and interstar connection.

3. Force Characteristics of the Support Model

3.1. Model Stress Duration Curve. According to the existing literature [23], after 50 days of forming, the self-shrinkage of the concrete tends to stabilize, so the influence of the self-shrinkage of the concrete during the model test on the results can be excluded. Therefore, the indoor test is carried out after the 54th day of pouring the lining. The room temperature was 15°C. After the lining model was placed indoors for 3 days, it was the same as the room temperature. It can be assumed that the inside of the model is a uniform steady-state temperature field and the temperature difference between the inner and outer walls is 0°C. Before the model starts to heat, the 24 strain gauges are rebalanced to zero to be able to consider the time when heating starts as the starting point of the recording of measurement data, measure the temperature strain value of the lining model during the whole test, and convert the stress value under different temperature differences. The duration curve is shown in Figure 9.

3.1.1. Warming Stage. Since the conduction of thermal energy in the model is slow, the literature [24] believes that the strain of cement-based materials such as concrete always lags behind the change of its temperature, and the changes in the two are not synchronized. At the same time, it takes a certain time to form an effective heat source, so the stress value measured at each measuring point of the model is small up to 200 s after the start of heating. As the heating progresses, the model thermal temperature stress begins to increase gradually after 500 s, and the higher the set heating temperature is, the faster the stress growth rate is.

3.1.2. Water Stage. The water (water temperature is 0°C) stage begins at 1500 s. The outer wall of the model maintains the set temperature, and the cold water is poured into the model. Due to the convective heat transfer between the cold water and the inner wall, the temperature of the inner wall of the model suddenly drops, and the influence of large temperature drop and high temperature difference on the inner wall causes the compressive strain of the inner wall to decrease rapidly and gradually change to tensile strain. The larger the temperature difference is, the larger the strain reduction is and the faster the reduction rate is. After a temperature drop of 90°C on the inner wall of the model, the circumferential measurement value appears after the water is passed.

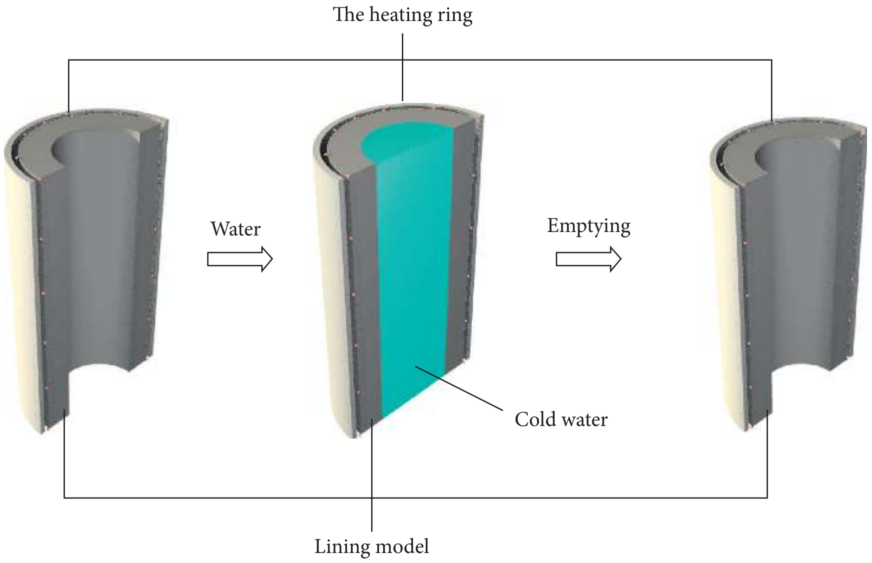

Figure 7: Process of experiment.

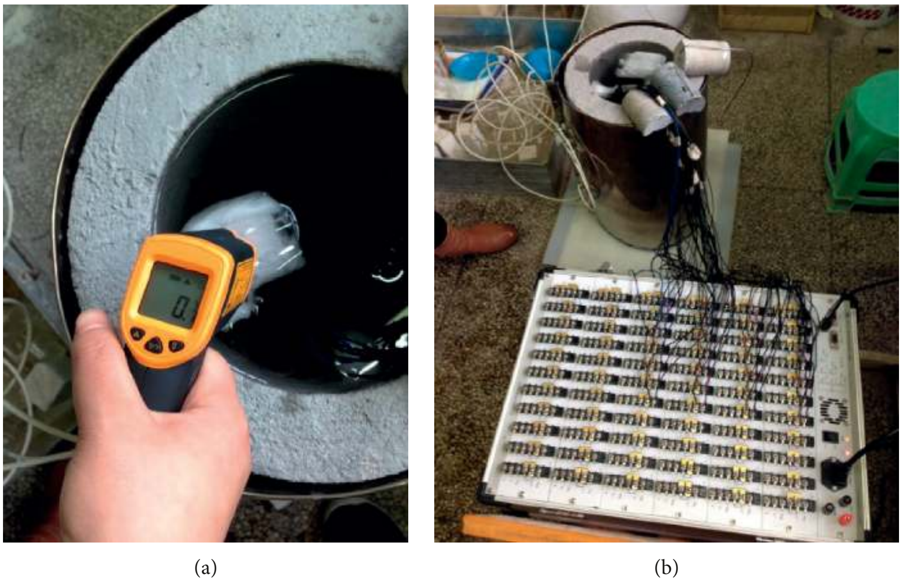
(a)
(b)

Figure 8: Heating excess cold water and test data sheet.

3.1.3. Venting Stage. After 1200 s of flowing water, and 2700 s later, the cold water was discharged from the model. At the initial stage of venting, the strain reduction rate gradually decreased, and the strain curve tended to be gentle. After the venting process continued, the strain value began to gradually increase towards the compressive strain, but the growth rate was still slow. After a temperature difference of 90°C, the circumferential tensile strain caused by the water is gradually reduced, and the transformation to compressive strain begins. Due to the short measurement time in the venting phase, the phenomenon of the compressive stress value returning to the prewater level was not measured.

The curve of the strain stress process curve when the water temperature is 10°C is similar to the curve when the water temperature is 0°C. Due to the difference between the strain value during the test and the final strain value after the water is discharged at 10°C, the temperature drop of the inner wall of the model is slightly smaller than that after water at 0°C. Therefore, the temperature stress change due to temperature drop is slightly smaller, the rate of change is slightly slower, and the hoop strain value is smaller under the influence of a large temperature drop.

3.2. Stress Characteristics of Support Model under Different Temperature Differences without Water. Figure 10 shows the temperature stress of the model under different temperature differences converted using the observed data of the upper, middle, and lower strain gauges as measured in the model. Under the condition of no water and under the different

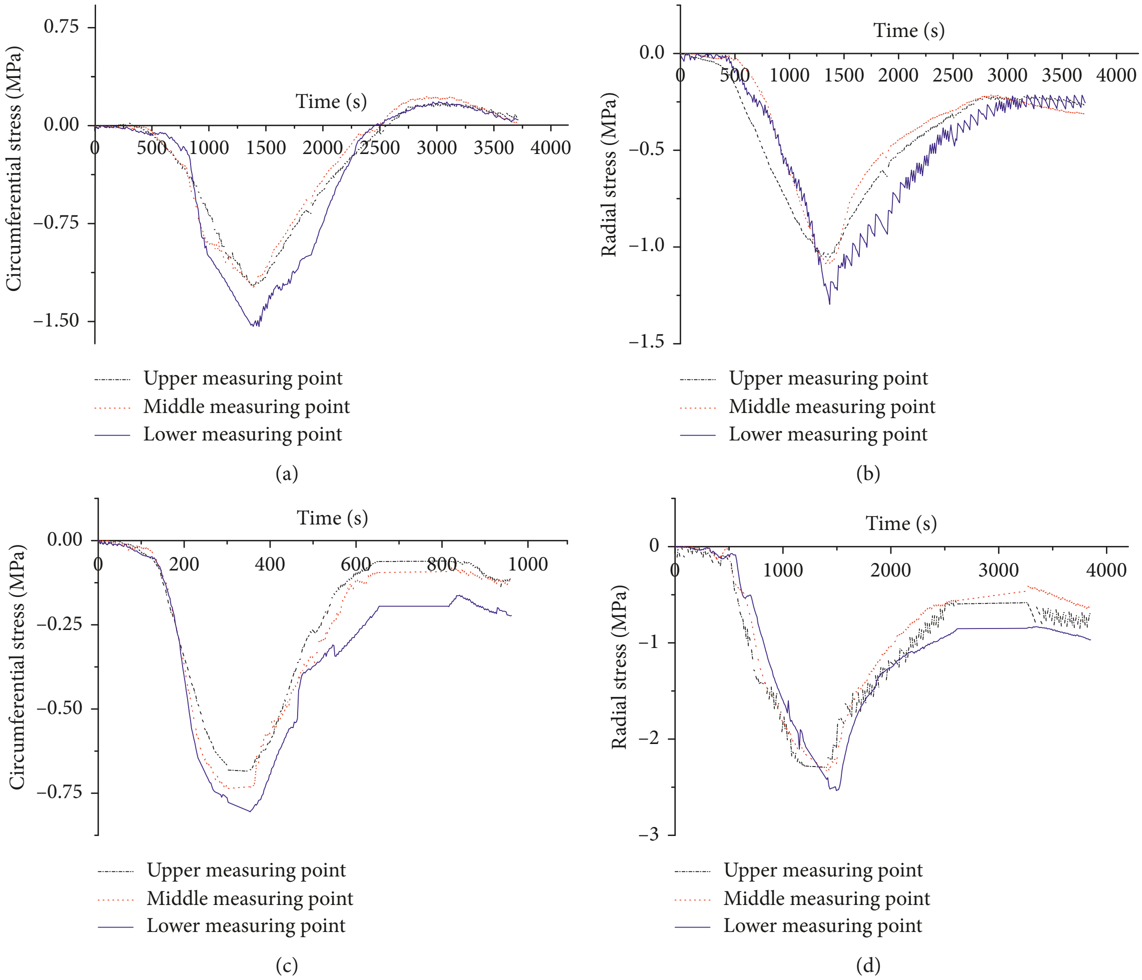

Figure 9: Stress curves for different heat source temperatures. (a) Circumferential stress: 90°C. (b) Radial stress: 90°C. (c) Circumferential stress: 60°C. (d) Radial stress: 60°C.

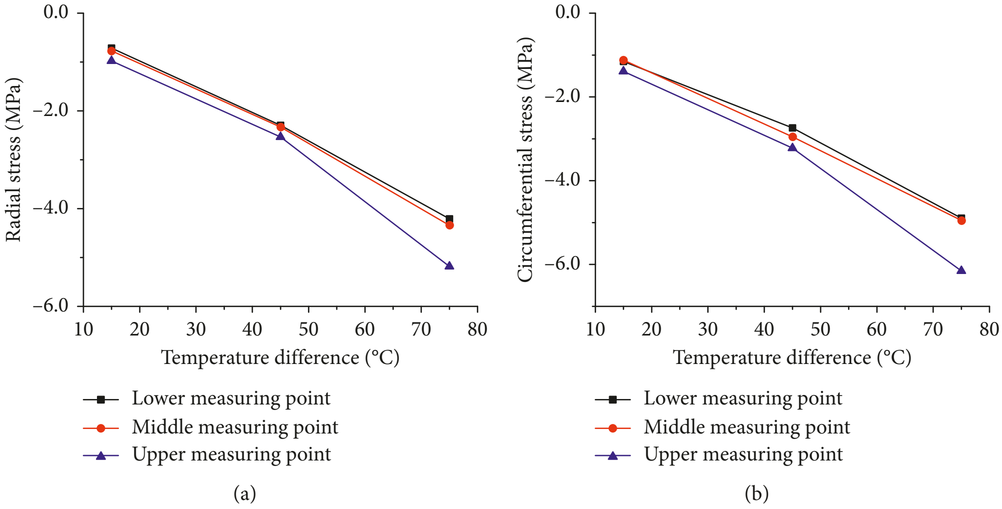

Figure 10: Maximum of thermal stress under different heating temperatures (0°C). (a) Radial stress. (b) Circumferential stress.

temperature differences between the inner and outer walls of the support structure, the temperature stress of the model has a significant effect. The greater the temperature difference is, the greater the temperature compressive stress values are at each observed point (in Figure 10, "–" means compressive stress), and the temperature difference and the stress have an approximately linear relationship. When the temperature of the heat source is 30°C, 60°C, and 90°C, that is, the temperature differences between the inner and outer walls of the support structure are 15°C, 45°C, and 75°C, respectively (the indoor temperature is 15°C), the maximum radial compressive stress is 5.18 MPa and the maximum circumferential temperature compressive stress is 6.15 MPa, as occurred in the upper observed position when the temperature difference is 75°C. The compressive stress of the support structure under the maximum temperature difference (75°C) is 5 to 6 times of that under the minimum temperature difference (15°C). At each value of temperature difference, the radial temperature stress is slightly less than the circumferential temperature stress. When the temperature differences between the inner and outer walls of the support structure are 15°C, 45°C, and 75°C, the circumferential temperature compressive stress at each position is ~10–60% larger than the radial temperature compressive stress. The reason is that, as the temperature of the outer wall of the model increases, the temperature difference between the inner and outer walls increases, thereby causing the circumferential deformation of the outer wall to be large and the inner wall to be low due to the low temperature. This causes the circumferential deformation to be small due to the circular constraint. Therefore, the compressive stress value is greater than the radial temperature compressive stress value.

3.3. *Stress Characteristics of Supporting Structure under Different Temperature Differences after Water Passes Through.*

To study the force of the supporting structure during the water passage period, the supporting model is filled with water under different temperatures to simulate the stress characteristics of the supporting structure under the operating conditions. According to the actual operation of the reservoir, it is determined that the water temperature is 0°C and 10°C. The outer wall of the support model is kept at the temperature of 30°C, 60°C, or 90°C.

In the water passage stage, the inner wall experiences a sudden drop in temperature due to contact with cold water. Under the influence of the high temperature difference caused by the large temperature drop, the compressive stress of the inner wall of the model decreases rapidly.

When the water temperature is 0°C, the temperature difference between the inner and outer walls of the model is 30°C, 60°C, and 90°C. The conversion stress value of various points of the model is shown in Figure 10.

As seen from Figure 11, the circumferential stress on the supporting structure converts from compressive stress ("−" value in the figure) to tensile stress ("+" value in the figure), with the increase in temperature difference (30°C, 60°C, and 90°C) caused by the water temperature of 0°C. When the temperature difference is 90°C, the tensile stress in the middle part of the support structure reaches the maximum of 0.89 MPa. The radial compressive stress is still the minimum compressive stress value of 0.16 MPa, and the state of stress does not change. When the temperature difference between the inner and outer walls is 90°C, the maximum compressive stress is 0.86 MPa. This is because when the temperature difference between the inner and outer walls is large, the circumferential deformation of the outer wall is large, causing the outer wall to be unconstrained, resulting in thermal expansion and excessive tensile stress.

When the water temperature is 10°C (Figure 12), the temperature stress at each observed point follows the same law as when the water is 0°C. The middle part of the support model produces a maximum tensile stress of 0.52 MPa in the circumferential direction at a maximum temperature difference of 80°C. When compared to the temperature difference of 90°C caused by 0°C water, the circumferential tensile stress is lower. The radial stress is still compressive stress, which is the minimum compressive stress of 0.20 MPa when the temperature difference between the outer and inner walls is 80°C and the maximum compressive stress is approximately 1.60 MPa. When compared with the temperature difference of 90°C caused by 0°C water, the value of radial compressive stress increases. When the water temperature is 10°C, the circumferential expansion deformation of the inner wall increases with the increase in temperature. Compared to the temperature difference caused by 0°C water, the difference between the circumferential expansion deformation values between the outer and inner walls decreases and the overall circumferential tensile stress decreases. The inward radial expansion deformation of the high temperature outer wall is greater than the outward expansion deformation of the inner wall, and a radial deformation develops towards the inner wall. Due to the inner wall constraint, a compressive stress is generated. When the inner wall temperature is low (0°C), due to the overall radial deformation, the distribution is adjusted within the entire thickness range of the support, causing the radial compressive stress to be small. In contrast, when the temperature of the inner wall rises to 10°C, the radial deformation is only distributed within the range of the thickness of the support, and thus the magnitude of the radial compressive stress increases.

The temperature drop in the inner wall of the model caused by water, which further caused the temperature compressive stress caused by the heating of the outer wall, was greatly reduced. The influence of water temperature on the temperature stress of the model explains the difference in the change of the value of stress. The lower the temperature of the water, the larger the temperature drop. The faster the stress changes, the greater the stress change will be.

The heating temperature of the outer wall was 30°C, 60°C, and 90°C, and the water temperature dropped from 10°C to 0°C, which means the temperature drop of the inner wall of the model goes from 20°C, 50°C, and 80°C to 30°C, 60°C, and 90°C, respectively. Change in the value of radial compressive stress was reduced by approximately 20%, 30%, and 15%, and change in the value of circumferential tensile stress increased by approximately 9%, 10%, and 15%, respectively.

It can be seen from the analysis of the stress characteristics of the support model when the water does and does not pass that for the support model, and there is a difference in the force change between the support models even under the same temperature difference. The reason for this is that

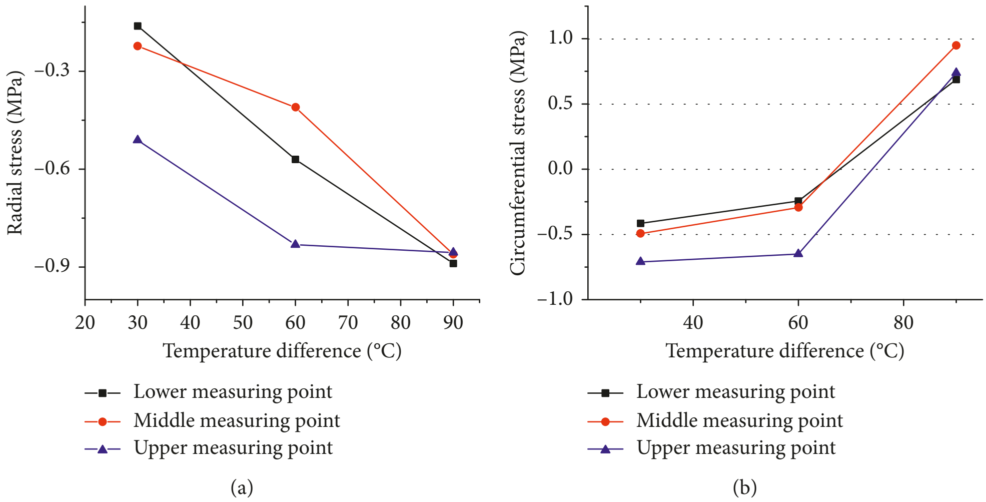

Figure 11: Maximum thermal stress under different heating temperatures. (a) Radial stress. (b) Circumferential stress.

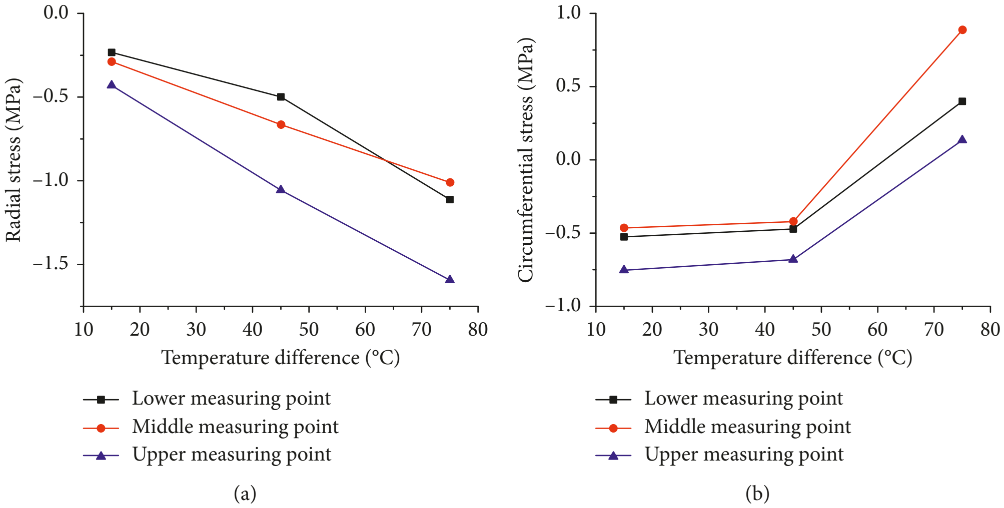

Figure 12: Maximum of thermal stress under different heating temperatures. (a) Radial stress. (b) Circumferential stress.

when the water does not pass, the temperature difference between the inner wall and the outer wall is determined by the temperature caused by the heater and room temperature. When the outer wall is heated to the desired temperature for a period of time (change moment of strain gauge as a standard), it is known that there is a temperature difference between the inner and outer walls, and the conversion stress measured at this time is the stress of the model under the temperature difference. However, when water is passed through the model, the actual situation is simulated, in which the entire support model is heated to high temperature for a period of time, and then the water is injected into the inner wall, resulting in a change in the internal force of the support structure caused by the rapid temperature difference. The former is a relatively slow process. In this process, there is no tensile stress, as there is no restraint, and the internal force is adjusted by itself. The latter is a rapid process, as the internal force is quickly adjusted and a large tensile stress occurs.

4. Comparative Analysis of the Numerical Model and Experiments

To further study the bearing characteristics of the lining support under different temperature differences, compared with the indoor model test, numerical experiments were carried out to analyze the stress variation law under different temperature differences. The numerical experimental model size is exactly the same as that of the indoor experimental model. The height of the model is 50 cm, the outer diameter is 30 cm, the inner diameter is 20 cm, and the radial thickness of the model is 5 cm. The model is divided by the unit of SOLID5 (scalar brick5) in ANSYS software. Model physical mechanics and thermodynamic parameters are shown in Table 2.

As seen from Figures 13 and 14, the experimental values and the calculated values show similar regularities: the higher the temperature of the heat source, the greater the change of the stress caused by the passage of water; under the

Table 2: Physical and thermodynamic parameters of the model.

Volumetric weight (kN/m^3)	Poisson's ratio	Elastic modulus (GPa)	Specific heat capacity J/(kg·°C)	Heat transfer coefficient W/(m·°C)	Convective heat transfer coefficient $W/(m^2 \cdot °C)$		Linear expansion coefficient 10–6/°C
					S-G	S-L	
19.9	0.167	5.2	960	8.8	4.74	600	11.2

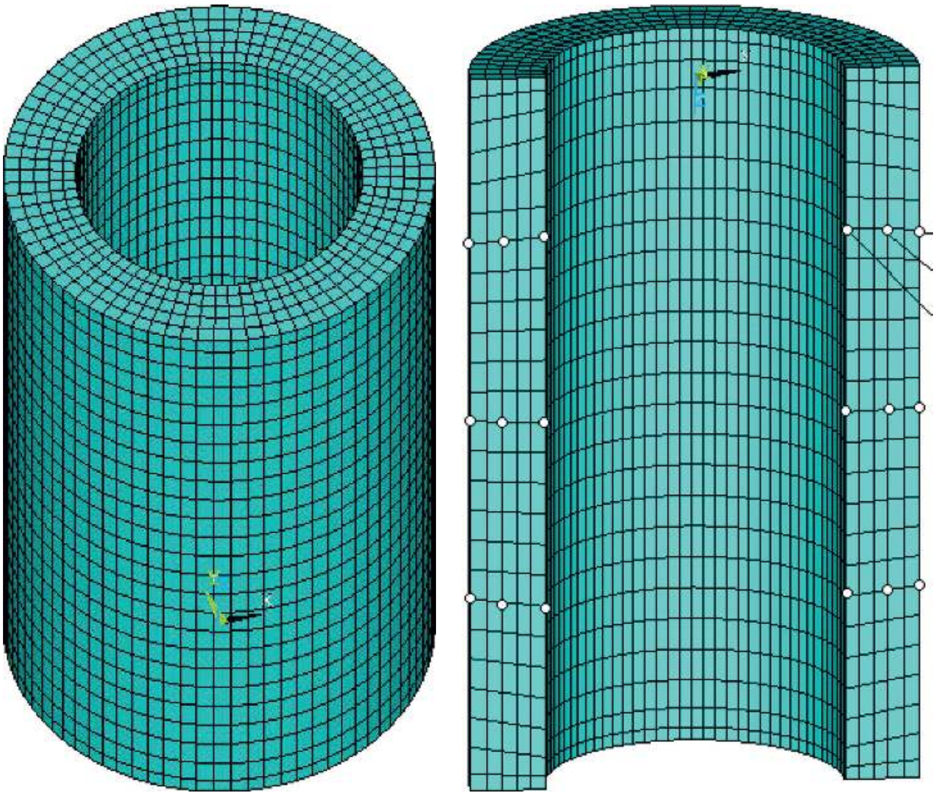

(a)

(b)

Figure 13: FEM model and element mesh.

same heat source temperature, the lower the water temperature, the greater the change value of the stress. The radial stress change values are less than those in the circumferential direction, which is similar to the stress change rule of the lining structure of the #2 test tunnel. In the model test, the change value of circumferential stress is approximately 1.2–1.8 times that of radial stress, and the value of circumferential stress in numerical calculation is approximately 2.1–2.3 times of that of radial stress. The change value of stress in the numerical calculation is slightly larger.

5. Discussion and Conclusion

(1) When there is a high temperature difference between the inner and outer walls of a tunnel lining support structure, large temperature stress will be generated inside the tunnel lining support structure. When water does not pass through, the inner and outer walls of the tunnel lining support structure have a temperature difference, the structure produces compressive stress, and the change value of temperature compressive stress is positively correlated with the temperature difference. The circumferential temperature compressive stress of the lining structure is 0.6 to 0.8 times that of the temperature difference. That is, the change time of temperature difference at the maximum temperature difference (75°C) is seven times that of the minimum temperature difference (15°C) in the model test, and the compressive stress value of the supporting structure is 5–6 times of that at the minimum temperature difference (15°C). At each value of temperature difference, the radial temperature stress is slightly less than the circumferential temperature stress. The circumferential temperature compressive stress is approximately 10–60% larger than the radial temperature compressive stress.

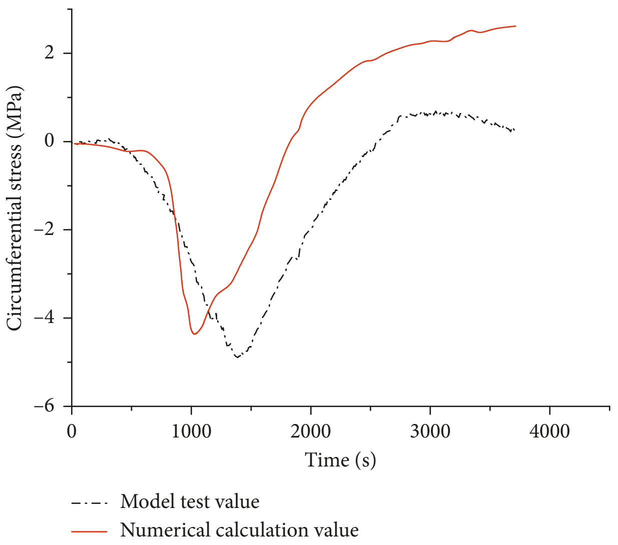

Figure 14: Curve of thermal stress of the middle layer in the simulation model.

(2) After the injection of water, the compressive stress value of the supporting structure decreases greatly and develops into tensile stress. In addition, the larger the temperature difference, the greater the decrease in stress caused by the change of temperature. When the water temperature is 0°C, the radial temperature compressive stress decreases by 48–80% when the temperature difference is 30°C, 60°C, and 90°C. When the water temperature is 10°C, the radial compressive stress decreases by 50–75%. The greater the temperature drop caused by the water, the greater the decrease of the temperature compressive stress. Radial temperature stress decreases less than the circumferential stress, and the radial temperature stress decreases to near zero.

(3) Under the condition of temperature drop caused by the passage of water, when the temperature drop of 90°C occurs on the inner wall of the support structure model, the circumferential stress at each position of the support model changes from compressive stress to tensile stress, and the maximum tensile stress is 0.89 MPa. When a temperature drop of 80°C occurs on the inner wall of the model, the circumferential stress at each location changes from compressive stress to tensile stress, and the maximum tensile stress is 0.52 MPa.

(4) The effect of water temperature on the temperature stress of the model is shown as the difference in the change value of the stress. The lower the temperature of the water is, the larger the temperature difference is. The faster the stress changes, the greater the stress changes. When water temperature is dropped from 10°C to 0°C, the radial compressive stress increases by 45–50% and the circumferential tensile stress increases by 40–60%. For high-temperature rock tunnels, the temperature difference between the inner and outer walls of the supporting structure caused by water temperature will cause large circumferential tensile stress.

(5) The general rules of the model test and numerical experiment are the same, and the same as the field test rule of #2 test hole. The numerical calculation results show that the change of stress is smaller than that of the indoor test, but the ratio of the change of circumferential stress to the change of radial stress is larger than that of the indoor test. The reason is that they are caused by different constraints.

Data Availability

The data used to support the findings of this study are available from the corresponding author upon request.

Conflicts of Interest

The authors declare that they have no conflicts of interest.

Acknowledgments

The authors gratefully acknowledge the financial supports provided by the National Science Foundation of China (Grant nos. 11572246 and 51179153). In addition, the work was supported by the Natural Science Foundation of Shaanxi Provincial Department of Education (Grant no. 15JK1540).

References

[1] F. Wang, M. Wang, and J. Huo, “The effects of the passive fire protection layer on the behavior of concrete tunnel linings: a field fire testing study,” *Tunnelling and Underground Space Technology*, vol. 69, pp. 162–170, 2017.

[2] J. Guo, S. P. Jiang, and Z. Y. Zhang, “Fire thermal stress and its damage to subsea immersed tunnel,” in *Proceedings of the 2nd International Symposium on Submerged Floating Tunnels and Underwater Tunnel Structures (SUFTUS), DEC*, vol. 166, pp. 296–306, Procedia Engineering, Chongqing, China, 2016.

[3] S.-n. Gu, G.-q. Zhu, and W.-x. Zan, “Numerical study on transverse temperature distribution of fire zone in metro tunnel fire,” in *Proceedings of the 2015 International Conference on Performance-based Fire and Fire protection Engineering(ICPFFPE2015)*, vol. 135, pp. 376–383, Procedia Engineering, Guangzhou, China, 2016.

[4] H.-p. Lai, S.-y. Wang, and Y.-l. Xie, “Experimental research on temperature field and structure performance under different lining water contents in road tunnel fire,” *Tunnelling and Underground Space Technology*, vol. 43, pp. 327–335, 2014.

[5] J. Rutqvist, D. Barr, Birkholzer et al., “Results from an international simulation study on coupled thermal, hydrological, and mechanical processes near geological nuclear waste repositories,” in *Proceedings of the International High-Level Radioactive Waste Management Conference*, vol. 163, pp. 101–109, Las Vegas, NV, USA, 2008.

[6] L. Duris and J. Aldorf, “Valuation of the Klimkovice Tunnel secondary lining temperature measurement results,” in *Proceedings of the 11th International Conference on Underground Construction*, Prague, Czech Republic, June 2010.

[7] M. Li, W. H. Chen, and W. Jia, “Calculation and analysis of the tunnel lining’s thermal stress field under high temperature,” in *Proceedings of the International Conference on Civil*

Engineering and Transportation (ICCET 2011) OCT 14-16, 2011, vol. 90-93, pp. 2157–2011, Applied Mechanics and Materials, Jinan, China, 2011.

[8] Y. Zhang, N. Li, and H. B. Zhang, "Study on splitting tensile strength of shotcrete layer of high temperature tunnel," in *Proceedings of the Global Conference on Civil, Structural and Environmental Engineering/3rd International Symp on Multi-field Coupling Theory of Rock and Soil Media and its Applications, China Three Gorges Univ*, pp. 594–597, Advances in Industry and Civil Engineering, PTS 1-4 Advanced Materials Research, Yichang, China, 2012.

[9] N. F. Liu, N. Li, J. P. Liu et al., "Mechanical characteristics of high-temperature tunnel based on analytical method," in *Proceedings of the 3rd International Society-for-Rock-Mechanics (ISRM) SINOROCK Symposium, Tongji University*, pp. 601–606, Rock Characterization, Modeling and Engineering Design Methods, Shanghai, China, June 2013.

[10] T. Wang, G. Zhou, J. Wang, and X. Zhao, "Stochastic analysis for the uncertain temperature field of tunnel in cold regions," *Tunnelling and Underground Space Technology*, vol. 59, pp. 7–15, 2016.

[11] J. Hu, B. S. Jiang, H. Zeng, Y. N. Chen, and Y. Y. Zhu, "Temperature field numerical analysis of different freeze pipe spacing of vertical frozen soil wall reinforcement at shield shaft," *Applied Mechanics and Materials*, vol. 580–583, pp. 738–741, 2014.

[12] C. S. Zhu and X. H. Yang, "Tunnel collapse treatment technique Research in Xinjiang Tianshan high-altitude, low-temperature Mountain," *Applied Mechanics and Materials*, vol. 580–583, pp. 1161–1167, 2014.

[13] X. Tan, W. Chen, G. Wu, and J. Yang, "Numerical simulations of heat transfer with ice-water phase change occurring in porous media and application to a cold-region tunnel," *Tunnelling and Underground Space Technology*, vol. 38, pp. 170–179, 2013.

[14] A. E. Bond, I. Brusky, N. Chittenden et al., "Development of approaches for modelling coupled thermal-hydraulic-mechanical-chemical processes in single granite fracture experiments," *Environmental Earth Sciences*, vol. 75, 2016.

[15] T. S. Nguyen, L. Börgesson, M. Chijimatsu et al., "A case study on the influence of THM coupling on the near field safety of a spent fuel repository in sparsely fractured granite," *Environmental Geology*, vol. 57, no. 6, pp. 1239–1254, 2009.

[16] J. Rutqvist, D. Barr, J. T. Birkholzer et al., "A comparative simulation study of coupled THM processes and their effect on fractured rock permeability around nuclear waste repositories," *Environmental Geology*, vol. 57, no. 6, pp. 1347–1360, 2009.

[17] C.-F. Tsang, O. Stephansson, L. Jing, and F. Kautsky, "DECOVALEX project: from 1992 to 2007," *Environmental Geology*, vol. 57, no. 6, pp. 1221–1237, 2009.

[18] J. Pacovsky, J. Svoboda, and R. Vasicek, "The effects of long-term thermal load on lining stability," in *Proceedings of the International Symposium on Geotechnics and Geotechnics-From Micro to Macro*, Shanghai, China, 2011.

[19] M. Lei, L. Peng, and C. Shi, "Model test to investigate the failure mechanisms and lining stress characteristics of shallow buried tunnels under unsymmetrical loading," *Tunnelling and Underground Space Technology*, vol. 46, pp. 64–75, 2015.

[20] C. Molins and O. Arnau, "Experimental and analytical study of the structural response of segmental tunnel linings based on an in situ loading test," *Tunnelling and Underground Space Technology*, vol. 26, no. 6, pp. 764–777, 2011.

[21] X. C. Yao, *Research on Thermal Stress Characteristics of Tunnel Surrounding Rock and Lining Structure under High Temperature Difference*, Xi'an University of Technology, Xi'an, China, 2013.

[22] X. Cai, G. Swobodag, W. Chen et al., "Safety design of tunnel lining in fire," *Chinese Journal of Rock Mechanicals Engineering*, vol. 29, no. S2, pp. 3805–3811, 2010.

[23] S. Li, *Research on Dry Shrinkage of Cement Mortar*, Nanjing University of Technology, Nanjing, China, 2004.

[24] F. Gu, *Research on Temperature Strain Test and Anti-Crack Measures of Mass Concrete*, Xi'an University of Architecture and Technology, Xi'an, China, 2005.


Journal of
Engineering
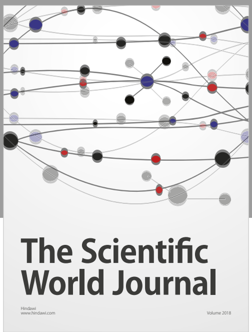
The Scientific
World Journal
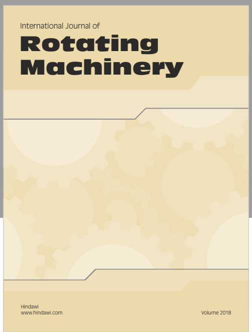
International Journal of
Rotating
Machinery

Journal of
Sensors
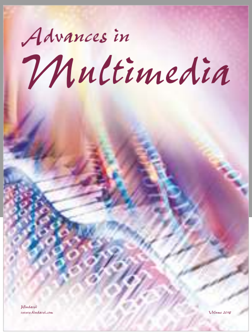
Advances in
Multimedia
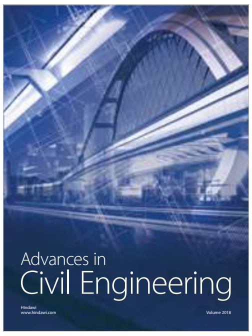
Advances in
Civil Engineering

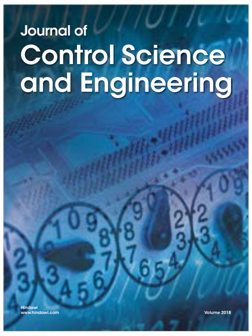
Journal of
Control Science
and Engineering

Journal of
Robotics

Journal of
Electrical and Computer
Engineering
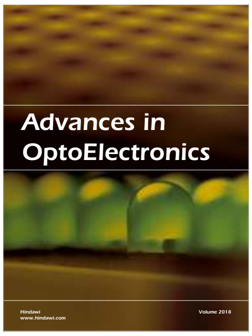
Advances in
OptoElectronics

VLSI Design

International Journal of
Navigation and
Observation
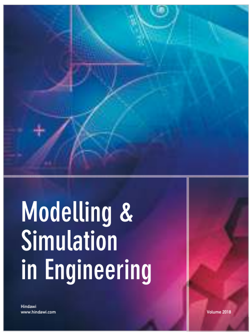
Modelling &
Simulation
in Engineering

International Journal of
Aerospace
Engineering

International Journal of
Chemical Engineering
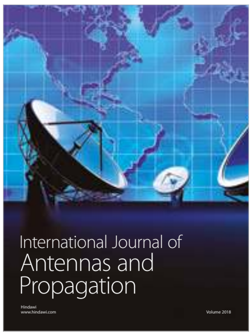
International Journal of
Antennas and
Propagation

Active and Passive
Electronic Components
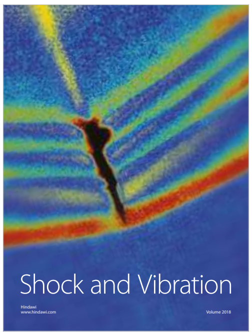
Shock and Vibration
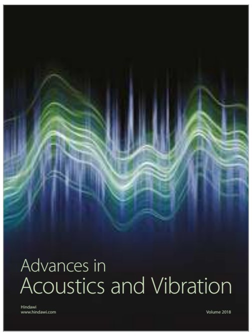
Advances in
Acoustics and Vibration